Kinetically controlled self-assembly of Rh(II)-based squares assisted by monotopic ligand

Atsushi Okazawa,[1†] Naoki Sanada[2†] and Shuichi Hiraoka[*2]

[1]Department of Electrical Engineering and Bioscience, Waseda University, Tokyo 169-8555, Japan

[2]Department of Basic Science, Graduate School of Arts and Sciences, The University of Tokyo, Tokyo 153-8902, Japan.

*Correspondence: hiraoka-s@g.ecc.u-tokyo.ac.jp

† These authors contributed equally.

Abstract

Self-assembled coordination squares consisting of *cis*-protected dinuclear Rh(II) corner complexes and linear ditopic ligands were selectively produced in solution under kinetic control with the assistance of a weak monotopic carboxylate ligand (2,6-dichlorobenzoate: dcb$^-$) as a leaving ligand. Preventing the cyclization step in the triangular formation by the leaving ligand enabled to produce the molecular square only. It was also found that dcb$^-$ can selectively convert the triangular complex into the square complex at room temperature, though heating at 373 K for 2 days is needed for the conversion without dcb$^-$ and that DMSO blocked the transformation process with dcb$^-$. These results indicate that the energy landscape of the Rh(II)-based molecular self-assembly can be modulated properly by monotopic carboxylate ligand and solvent so that the self-assembly proceeds under kinetic control. Furthermore, one of the molecular squares assembled into a dimeric structure by the solvophobic effect, whose structure was characterized by NMR spectroscopy and single-crystal X-ray analysis.

Introduction

Molecular square is one of the most representative molecular architectures in coordination self-assembly.[1–21] Thanks to 90° of the L–M–L bond angle provided by octahedral and square planer transition metal ions, square complexes are thermodynamically most stable over other polygonal structures such as a triangular complex. However, as a matter of fact, corresponding triangular complexes are often coproduced in solution even in the case where linear ditopic ligands that act as the side of the polygons are rigid,[22–42] so the selective formation of molecular squares and understanding of its origin are still a challenging topic in supramolecular chemistry.[43]

There are two strategies to produce molecular squares selectively. If the molecular square is more stable than the other products with large enough energy differences, the square is produced as a single product under thermodynamic control (Fig. 1a). What is required in this case is to provide high reversibility of M–L coordination bonds as seen in Pd(II)–N and Zn(II)–N bonds so that the self-assembly reaches equilibrium (global reversibility in the system).

When the energy difference between the square and the triangle is small, even if the molecular square is thermodynamically most stable, the molecular triangle cogenerates under thermodynamic control (Fig. 1b). In the case where reversibility of M–L coordination bond is not so high, the metastable triangle is kinetically so stable that its conversion to the thermodynamically most stable square is prevented (Fig. 1c). In such a case, the square complex should be selectively produced by pathway selection, inhibiting the triangular formation under kinetic control. Such a kinetic approach is rare in molecular self-assembly except unexpected observation of kinetic traps.[44–52] As far as we know, there is no report on the selective formation of a triangular or square complex under kinetic control.

Cotton and his co-workers and others reported that molecular squares composed of *cis*-protected dinuclear Rh(II) complexes (***Rh***$^{2+}$: $[Rh_2(DAniF)_2]^{2+}$ [53] and $[Rh_2(O_2C\text{-}R\text{-}CO_2)]^{2+}$ [54]) and linear dicarboxylates (L^{2-}) were selectively obtained in crystalline states.[53,54] As Rh(II)–carboxylate coordination bonds in dinuclear Rh(II) complexes are relatively strong, the reversibility of the coordination bond is not high,[55] which would let the self-assembly of the ***Rh***$_4$L$_4$ squares proceed under kinetic control. Thus, we are interested in why the ***Rh***$_4$L$_4$ squares were selectively produced in the solid state in the previous research and how to selectively form the ***Rh***$_4$L$_4$ squares under kinetic control in solution by modulation of the energy landscape.

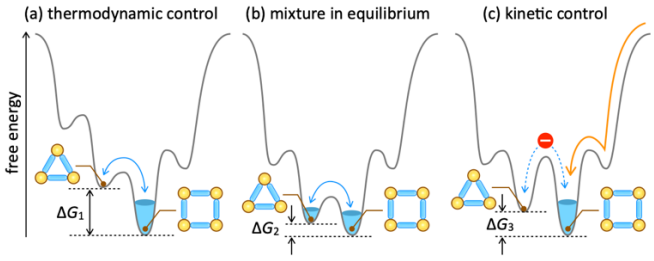

Figure 1. Schematic representation of energy landscapes of self-assembly of thermodynamically most stable M_4L_4 square and metastable M_3L_3 triangular complexes. (a) When the free energy difference between M_4L_4 and M_3L_3, ΔG_1, is large, M_4L_4 is exclusively produced under thermodynamic control. (b) When the energy difference, ΔG_2, is small, M_4L_4 and M_3L_3 are produced under thermodynamic equilibrium (Boltzmann distribution). (c) When the energy barriers of the conversion between M_4L_4 and M_3L_3 are so high that they are not interconvertible under self-assembly condition, M_4L_4 can be selectively produced by pathway selection under kinetic control (orange arrow) regardless of the energy difference ΔG_3.

Herein, we report the selective self-assembly of the ***Rh***$_4$L$_4$ squares in solution under kinetic control by using a weak monotopic carboxylate (2,6-dichlorobenzoate: dcb$^-$) as the leaving ligand to properly modulate the free energy landscape (Fig. 2). Without dcb$^-$ in the Rh(II) metal source, triangular and square complexes were produced in solution. When dcb$^-$ was used as the leaving ligand, the ***Rh***$_4$L$_4$ squares were obtained without formation of the ***Rh***$_3$L$_3$ triangles during the self-assembly. It was also found that the ***Rh***$_3$L$_3$ triangles were transformed into the ***Rh***$_4$L$_4$ squares at room temperature by

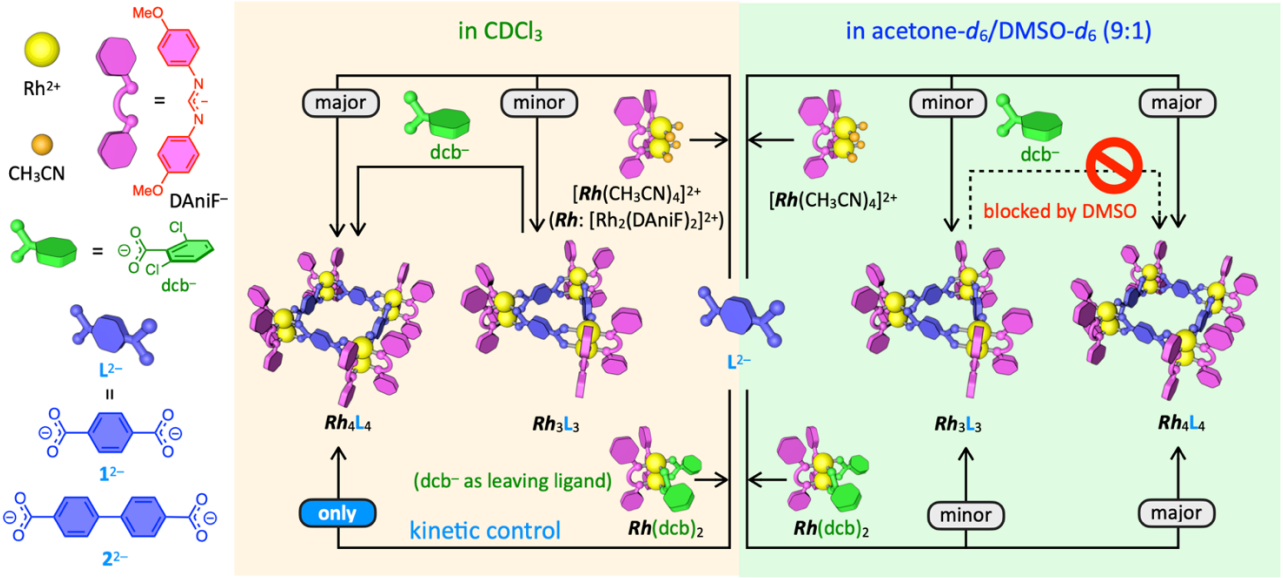

Figure 2. Schematic representation of kinetically controlled self-assembly of the ***Rh***$_4$L$_4$ squares in solution. The axial ligands on the Rh(II) centers are omitted for clarity.

addition of dcb⁻. This assist effect of dcb⁻ was perfectly blocked by 10 volume% of DMSO in solvent. The self-assembly process of the ***Rh***$_4$L$_4$ square was investigated experimentally to discuss why the ***Rh***$_4$L$_4$ square was selectively assembled with dcb⁻ under kinetic control. Furthermore, one of the ***Rh***$_4$L$_4$ squares aggregates to form a supramolecular dimer by the solvophobic effect.

Results and discussion

Self-assembly of Rh(II)-triangle and square with CH$_3$CN as a leaving ligand

We first carried out the self-assembly from [***Rh***(CH$_3$CN)$_4$](BF$_4$)$_2$ and **1**$^{2-}$ in CH$_3$CN ([**1**$^{2-}$] = 10 mM) according to the literature.[53] Dark red solid was precipitated in 1 day. Its ^{1}H NMR spectrum in CDCl$_3$ showed two prominent singlet signals of H^d (aromatic protons of **1**$^{2-}$ (Fig. 3)) in a 1:3 integral ratio, suggesting the formation of two highly symmetric cyclic structures (Fig. S1). Crystallization of this mixture in CHCl$_3$ gave single crystals of the ***Rh***$_4$**1**$_4$ square as was reported.[53] The major ^{1}H NMR signals are the same as those of the ***Rh***$_4$**1**$_4$ square (Fig. S2), so the minor signals are expected to correspond to the ***Rh***$_3$**1**$_3$ triangle, which was supported by ^{1}H DOSY spectroscopy (Fig. S3). Therefore, the ***Rh***$_4$**1**$_4$ square and the ***Rh***$_3$**1**$_3$ triangle were produced in CH$_3$CN.

To deeply investigate the solution process, the self-assembly was carried out in CDCl$_3$ at 298 K ([**1**$^{2-}$] = 1.0 mM). It was found that a mixture of the ***Rh***$_3$**1**$_3$ triangle and the ***Rh***$_4$**1**$_4$ square in a 1:2 ratio was obtained (Fig. 3a). Similarly, the self-assembly of [***Rh***(CH$_3$CN)$_4$](BF$_4$)$_2$ and another ditopic ligand (**2**$^{2-}$) in CDCl$_3$ gave the triangular and square complexes in a 1:2 ratio (Figs. S2, S4, and S5). Heating a 1:2 mixture of the ***Rh***$_3$**1**$_3$ triangle and the ***Rh***$_4$**1**$_4$ square in CDCl$_3$ at 60 °C did not show any change except slight broadening of the ^{1}H NMR spectrum (Fig. S6a). Heating the mixture in dimethylacetamide (DMA) at 100 °C for 2 days afforded the ***Rh***$_4$**1**$_4$ square as a solo product (Fig. S6b). This result indicates that the ***Rh***$_4$**1**$_4$ square is thermodynamically most stable and that heating at high temperature (100 °C) for long time is necessary for the conversion of the triangle into the square. Consequently, the self-assembly of [***Rh***(CH$_3$CN)$_4$]$^{2+}$ and linear ditopic ligands (L^{2-}) at room temperature gave a mixture of molecular triangle and square in solution and the ***Rh***$_4$**1**$_4$ square was selectively crystalized from the mixture in the previous report.

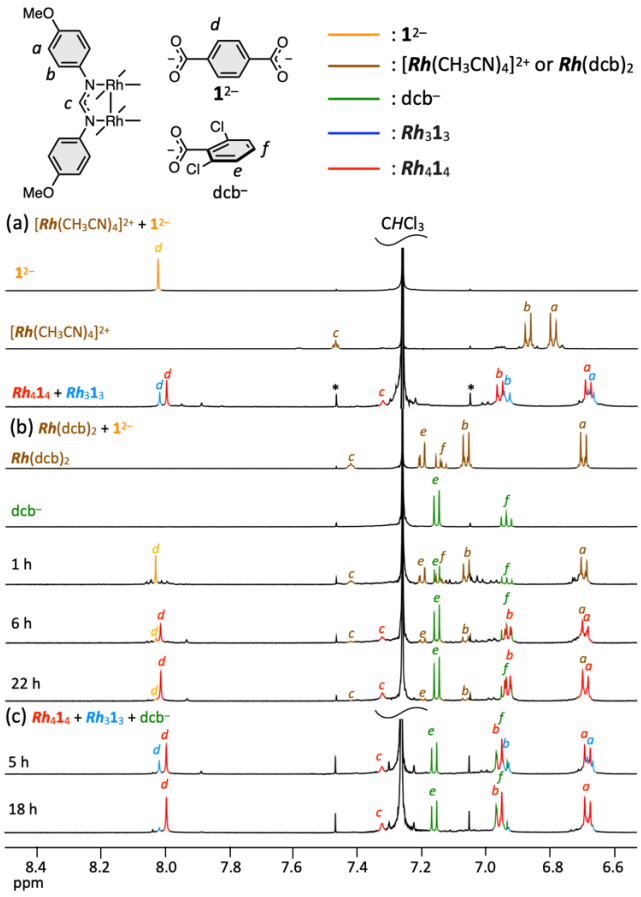

Figure 3. ^{1}H NMR spectra (500 MHz, CDCl$_3$, 298 K, aromatic region) of the self-assembly of the ***Rh***$_4$L$_4$ squares under various conditions ([**1**$^{2-}$] = [***Rh***$^{2+}$] = 1 mM). (a) Self-assembly from [***Rh***(CH$_3$CN)$_4$](BF$_4$)$_2$ and **1**$^{2-}$ in CDCl$_3$ at 298 K, giving the ***Rh***$_3$**1**$_3$ triangle and the ***Rh***$_4$**1**$_4$ square in 23 and 39%, respectively. (b) Self-assembly of the ***Rh***$_4$**1**$_4$ square from ***Rh***(dcb)$_2$ and **1**$^{2-}$ in CDCl$_3$ at 298 K to produce the ***Rh***$_4$**1**$_4$ square in 65% without formation of the ***Rh***$_3$**1**$_3$ triangle during the self-assembly. The yields were determined based on the internal standard. (c) Addition of *n*-Bu$_4$N·dcb in a mixture of the ***Rh***$_3$**1**$_3$ triangle and the ***Rh***$_4$**1**$_4$ square obtained from the self-assembly of [***Rh***(CH$_3$CN)$_4$](BF$_4$)$_2$ and **1**$^{2-}$ in CDCl$_3$ after the convergence. The ***Rh***$_3$**1**$_3$ triangle was converted into the ***Rh***$_4$**1**$_4$ square at 298 K assisted by dcb⁻, though heating at 100 °C for 2 days is necessary without dcb⁻ (see Fig. 6).

Selective self-assembly of Rh(II)-squares with the aid of leaving ligand

It was previously reported that the ligand exchange concerning Rh(II)–carboxylate bonds takes place through associative process like Pd(II)–N coordination donds.[56,57] In our previous research on Pd(II)-based coordination self-assemblies, the leaving ligand contributes to the modulation of the free energy landscape, resulting in changing the self-assembly pathway and the outcome.[58,59] We then investigated the kinetic effect of the leaving ligand on the ***Rh***-based self-assembly. 2,6-dichlorobenzoate (dcb^-) was chosen as the leaving ligand (Fig. 2). As the pK_a value of Hdcb in H_2O (1.82)[60,61] is lower than that of those of the ditopic ligands (L^{2-}), dcb^- would act as a leaving ligand. To test the potential of dcb^- as a leaving ligand, the ligand exchange of dcb^- in ***Rh***$(dcb)_2$ with *p*-toluate (tol^-) in $CDCl_3$ was monitored by ^{1}H NMR spectroscopy (Fig. S7a). The ligand exchange took place at 298 K to produce ***Rh***$(tol)_2$ in 82 % yield (Fig. S7b), indicating that dcb^- can be used as a leaving ligand in ***Rh***-based self-assembly at room temperature.

The self-assembly of ***Rh***$(dcb)_2$ and L^{2-} ($\mathbf{1}^{2-}$ and $\mathbf{2}^{2-}$) in $CDCl_3$ at 298 K was monitored by ^{1}H NMR spectroscopy (Figs. 3b and S8). Surprisingly, it was found that the signals of the ***Rh***$_3$L$_3$ triangles did not appear during the self-assembly for $\mathbf{1}^{2-}$ and $\mathbf{2}^{2-}$ to produce the ***Rh***$_4$L$_4$ squares selectively. These results indicate that the formation of the ***Rh***$_3$L$_3$ triangles was kinetically prevented by modulation of the energy landscape of the self-assembly with dcb^- as a leaving ligand.

Self-assembly process of Rh(II)-squares

The self-assembly processes of the ***Rh***$_4$L$_4$ squares from ***Rh***$(dcb)_2$ and L^{2-} ($\mathbf{1}^{2-}$ or $\mathbf{2}^{2-}$) were investigated by QASAP (quantitative analysis of self-assembly process).[62-64] We have applied QASAP in Pd(II)- and Pt(II)-based coordination self-assemblies. QASAP of the ***Rh***$_4$L$_4$ squares is the first example of the investigation of the self-assembly process for metal-organic assemblies with transition metal centers other than Pd(II) and Pt(II) ions.

In QASAP of the ***Rh***$_4$L$_4$ squares, the substrates (***Rh***$(dcb)_2$ and L^{2-}) and the products (***Rh***$_4$L$_4$ and dcb^-) were quantified by ^{1}H NMR spectroscopy (Fig. 4b), and the change in the average composition of all intermediates with time was plotted in a 2D map (*n*-*k* map) (Fig. 4c). The species regarding the self-assembly are expressed by ***Rh***$_a$L$_b$$(dcb)_c$ (*a*–*c* are 0 or positive integer). The (*n*, *k*) values of ***Rh***$_a$L$_b$$(dcb)_c$ are defined as $n = (2a - c)/b$ and $k = a/b$.[62-64] The *n* value indicates the average number of Rh^{2+} bound to a single ditopic ligand, L^{2-}, while the *k* value indicates the ratio between Rh^{2+} and L^{2-}. The experimentally obtained (*n*, *k*) values, which is indicated as ($\langle n \rangle$, $\langle k \rangle$), are calculated for the average composition of all intermediates (***Rh***$_{(a)}$L$_{(b)}$$(dcb)_{(c)}$), whose time-development was used for the discussion on the self-assembly process (Fig. 4c).

There are three types of chain intermediates with different in the terminals (Types I–III) (Figure 4a).[65,66] The (*n*, *k*) values of the three types of oligomers are plotted on different straight lines in the *n*-*k* map (Figure 4c). With increase in the oligomerization degree (*m* in Figure 4a), the (*n*, *k*) values become close to (2, 1), which is the (*n*, *k*) value of cyclic structures (triangle and square). Thus, the (*n*, *k*) plot enables us to discuss which type of oligomers were mainly produced and how large the chain-like oligomers grew during the self-assembly.

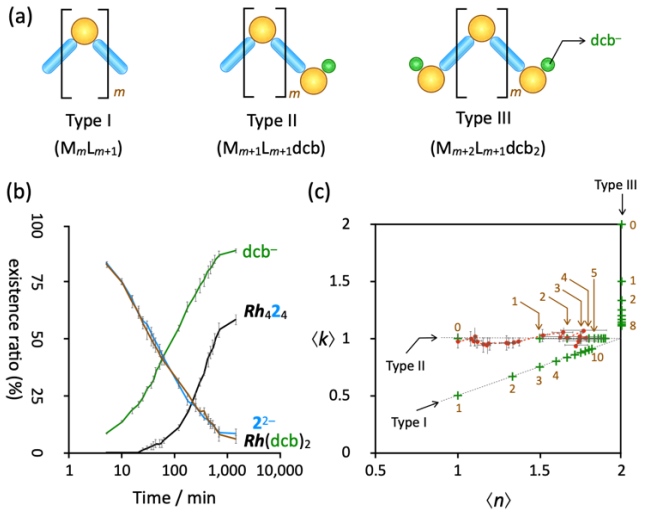

Figure 4. (a) Three types of possible chain intermediates in the self-assembly of M_4L_4 square. Type I: $M_mL_{(m+1)}$, Type II: $M_{(m+1)}L_{(m+1)}(dcb)$, Type III: $M_{(m+2)}L_{(m+1)}(dcb)_2$. (b) Plots of the existence ratios of the substrates and products in the self-assembly of the ***Rh***$_4$**2**$_4$ square from ***Rh***$(dcb)_2$ and $\mathbf{2}^{2-}$ in $CDCl_3$ at 298 K. $[Rh]_0 = [\mathbf{2}^{2-}]_0 = 0.86$ mM. (c) Plots of the ($\langle n \rangle$, $\langle k \rangle$) values in the *n*-*k* map of the ***Rh***$_4$**2**$_4$ square (red filled circles). Green crosshairs indicate the (*n*, *k*) values of chain intermediates. The three types of chain intermediates, Types I, II, and III, are plotted on each straight line. Brown number indicates *m* in each type of oligomer in (a). The definition of $\langle n \rangle$ and $\langle k \rangle$ values is shown in the main text and the Supplementary Information (equations S1 and S2).

As to QASAP for the ***Rh***$_4$**1**$_4$ square, the $\langle n \rangle$ value was smaller than 1 (Fig. S9 and Table S1), which suggests that Rh^{2+} units in the intermediates have more than two carboxylate ligands ($\mathbf{1}^{2-}$ and/or dcb^-), so further analysis could not be done (for detailed discussion, see Fig. S9). Such a strange behavior was not found for the self-assembly of the ***Rh***$_4$**2**$_4$ square (Figs. 4c and S10 and Table S2). The $\langle n \rangle$ value increased with almost constant $\langle k \rangle$ value of 1, indicating that the self-assembly took place mainly producing Type II oligomers as intermediates, whose *m* value finally reached 3 or 4, corresponding to 4 or 5 Rh^{2+} units in the oligomers.

Reason for the selective formation of Rh(II)-squares under kinetic control

Based on the result obtained by QASAP that Type II chain oligomers ***Rh***$_{m+1}$L$_{m+1}$(dcb) are major intermediates, the reason why the ***Rh***$_3$L$_3$ triangles were not produced when dcb^- was used as the leaving ligand is discussed. ***Rh***$_a$L$_b$$(dcb)_c$ is indicated as (*a*,*b*,*c*) for simplicity. There are two types of reactions to produce the ***Rh***$_3$L$_3$ triangle by cyclization of Type II intermediates: (1) The cyclization of (3,3,1) to form (3,3,0) through breaking the coordination bond between Rh(II) and the leaving ligand (CH_3CN or dcb^-) (Fig. 5a, left) and (2) the cyclization of longer oligomers than (3,3,1), (*m*+1, *m*+1, 1) ($m \geq 3$), by breaking a Rh–L coordination bond (Fig. 5a, right). The formation of the ***Rh***$_3$L$_3$ triangle from (*m*+1, *m*+1, 1) ($m \geq 3$) is not affected by the leaving ligand. The (*n*, *k*) plot of the self-assembly from ***Rh***$(dcb)_2$ and $\mathbf{2}^{2-}$ (Fig. 4c) indicates the formation of such long oligomers ($m \geq 3$). Therefore, the formation of the ***Rh***$_3$L$_3$ triangles from (*m*+1, *m*+1, 1) ($m \geq 3$) should be prevented and the cyclization of (3,3,1) to form (3,3,0) should also be prevented when dcb^- is the leaving ligand. In other words, the ***Rh***$_3$L$_3$ triangles is produced only through the cyclization of chain-like intermediate ***Rh***$_3$L$_3$$(CH_3CN)_2$ ((3,3,1) in Fig. 5a whose green sphere are two molecules of CH_3CN).

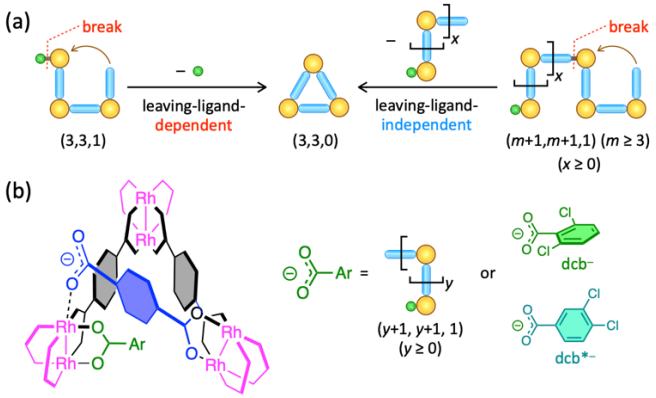

Figure 5. (a) Two possible pathways to produce the triangle (3,3,0) from Type II intermediates (3,3,1) (left) and from Type II oligomers with more than three ***Rh***$^{2+}$ units (m+1, m+1, 1) ($m \geq 3$) (right). Green sphere indicates the leaving ligand(s) (dcb$^-$ or two molecules of CH_3CN). (b) A plausible key structure in the triangular formation through associative process.

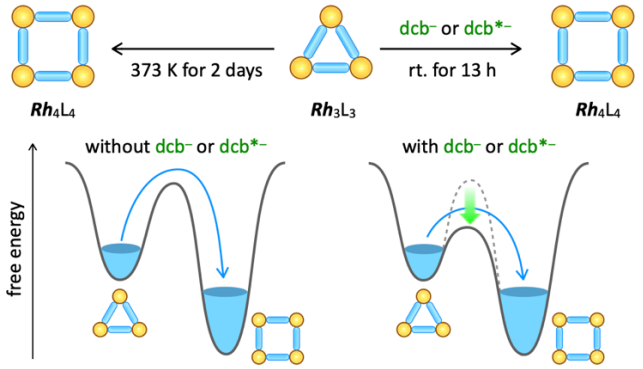

Figure 6. Transformation of the ***Rh***$_3$L$_3$ triangles into the ***Rh***$_4$L$_4$ squares is possible at rt. assisted by dcb$^-$ or dcb*$^-$, while heating at 373 K for 2 days is needed without dcb$^-$ or dcb*$^-$. The chemical structure of dcb*$^-$ is shown in Fig. 5b.

The benzene ring and carboxylate in dcb$^-$ are not planer due to steric repulsion around the two Cl atoms at 2 and 6 positions (Fig. 5b), which is different from the ditopic ligands, **1**$^{2-}$ and **2**$^{2-}$. To investigate the effect of planarity of benzoate ligands on the cyclization processes, the self-assembly was carried out with 3,4-dichlorobenzoate (dcb*$^-$) (Fig. 5b) as the leaving ligand. The coordination ability of dcb*$^-$ is lower than that of benzoate (pK_a of Hdcb* = 3.64).[60,61] As with dcb$^-$, the self-assembly from ***Rh***(dcb*)$_2$ and **1**$^{2-}$ gave the ***Rh***$_4$**1**$_4$ square without formation of the ***Rh***$_3$**1**$_3$ triangle during the self-assembly (Fig. S11). This result suggests that the triangular formation processes releasing a benzoate derivative (dcb$^-$ or ***Rh***$_{x+1}$L$_{x+1}$(dcb) (Fig. 5a, right)) are kinetically suppressed.

Considering the ligand exchange mechanism of Rh(II)–carboxylate bonds by associative process, the triangular formation should take place by the coordination of the free carboxylate in Type II intermediates to the axial site of a Rh(II) center (Fig. 5b). The instability of a cyclic intermediate or a transition state with a benzoate derivative (L^{2-}, dcb$^-$ and dcb*$^-$) as the leaving ligand would be the reason for the suppression of the ***Rh***$_3$L$_3$ triangles. In contrast, when the leaving ligand is CH_3CN (from [***Rh***$(CH_3CN)_4]^{2+}$), the ***Rh***$_3$L$_3$ triangles can be formed as a minor product.

Conversion of Rh(II)-triangles into Rh(II)-squares assisted by dcb$^-$

Considering the associative ligand exchange mechanism of Rh(II)-carboxylate bonds, the ligand exchange is expected to be facilitated by monotopic carboxylate with weak coordination ability such as dcb$^-$. Thus, n-Bu_4N·dcb was added in a mixture of ***Rh***$_3$**1**$_3$ and ***Rh***$_4$**1**$_4$ in $CDCl_3$, and the reaction at 298 K was monitored by ^{1}H NMR spectroscopy (Fig. 3c). The signals assigned to ***Rh***$_3$**1**$_3$ slowly decreased with time and almost disappeared in 18 h. Likewise, the conversion of ***Rh***$_3$**2**$_3$ into ***Rh***$_4$**2**$_4$ also took place at 298 K in 13 h (Fig. S12). These results indicate that dcb$^-$ efficiently converts the ***Rh***$_3$L$_3$ triangles into the ***Rh***$_4$L$_4$ squares under mild condition (room temperature), though heating at 100 °C for 2 days is needed for the conversion without dcb$^-$ as mentioned above, indicating that the energy barriers of the conversion of the ***Rh***$_3$L$_3$ triangles to the ***Rh***$_4$L$_4$ squares are largely lowered by dcb$^-$ (Fig. 6).

Solvent effect on kinetically controlled self-assembly

The rate of the self-assembly of the ***Rh***$_4$L$_4$ square was affected by solvent. It was found that the self-assembly from ***Rh***(dcb)$_2$ and **1**$^{2-}$ was largely retarded by addition of 10 volume% of DMSO in $CDCl_3$ solvent and that the ***Rh***$_4$**1**$_4$ square was not produced (Fig. S13). Slow release of free dcb$^-$ in the self-assembly indicates the inhibition of the ligand exchanges by DMSO. The color of the reaction mixture in $CDCl_3$/DMSO (9:1 (v/v)) (orange) is different from the green solution in $CDCl_3$, suggesting the coordination of S atom of DMSO to the axial site of Rh(II).[53,67,68] This idea was supported by the crystal structure of the ***Rh***$_4$**1**$_4$ square obtained from acetone/DMSO (Fig. 7b). The coordination of DMSO to the axial sites in ***Rh***$^{2+}$ would be the reason for the slow ligand exchange between carboxylate ligands. In contrast, the rate of the self-assembly in acetone-d_6/DMSO-d_6 (9:1 (v/v)) is similar to that in $CDCl_3$, though the color of the reaction mixture in acetone-d_6/DMSO-d_6 is orange (Figures S14 and S15). Acetone may compete with DMSO, which would diminish the blocking effect of DMSO on the ligand exchange.

The effect of DMSO on the conversion of the ***Rh***$_3$L$_3$ triangle into the ***Rh***$_4$L$_4$ squares assisted by dcb$^-$ was then investigated. The conversion of the ***Rh***$_3$L$_3$ triangles into the ***Rh***$_4$L$_4$ squares by dcb$^-$ was perfectly blocked in $CDCl_3$/DMSO-d_6 (9:1) (Figs. S16 and S17).

The triangle/square ratio was also affected by DMSO. The ***Rh***$_3$**L**$_3$ triangle and the ***Rh***$_4$**L**$_4$ square were produced in a 1:2 ratio from ***Rh***(dcb)$_2$ and L^{2-} (**1**$^{2-}$ or **2**$^{2-}$) in acetone-d_6/DMSO-d_6 (9:1 (v/v)) (Figs. S14 and S15). These results suggest that DMSO affects the stabilization of the intermediate(s) or the transition state(s) in the triangular formation process.

Supramolecular dimerization of Rh(II)-square by solvophobic effect

It was found that new set of signals appeared when the ***Rh***$_4$**1**$_4$ square was dissolved in $CD_3NO_2/CDCl_3$ (9:1 (v/v)) (Fig. 7c). Similar spectral change was observed in acetone-d_6 and CD_3CN with 10 volume% of $CDCl_3$ (Fig. S18). Significant up-field shift of aromatic protons (H^a and H^b) suggests the aggregation of the square (Fig. 7a). All the signals except for H^c were observed as two sets with a 1:1 integral ratio, which is consistent with the crystal structure of the [***Rh***$_4$**1**$_4$(dmso-*S*)$_4$]$_2$ dimer (Fig. 7b) obtained after the self-assembly in acetone-d_6/DMSO-d_6 (9:1 (v/v)) at 298 K.

The [***Rh***$_4$**1**$_4$]$_2$ dimer $CD_3NO_2/CDCl_3$ (9:1 (v/v)) was characterized by ^{1}H DOSY, (H, H)-COSY and (H, H)-NOESY spectroscopy (Figs. 7c, S19, and S20). A cross peak was found between H$^{a(out)}$ and H$^{a(in)}$ protons in the NOESY spectrum (Fig. S20), indicating the chemical exchange of the two proton signals caused by the rotation of the 1,4-

phenylene ring in $\mathbf{1}^{2-}$, which would be the reason for broadening of the two H^d signals (Fig. 7c). The monomer ($\boldsymbol{Rh}_4L_4$) and dimer ($[\boldsymbol{Rh}_4\mathbf{1}_4]_2$) equilibrium shifted towards the dimer with increase in the composition ratio of $CD_3NO_2/CDCl_3$ (Fig. S21), indicating the dimerization of the $\boldsymbol{Rh}_4\mathbf{1}_4$ square due to the solvophobic effect.

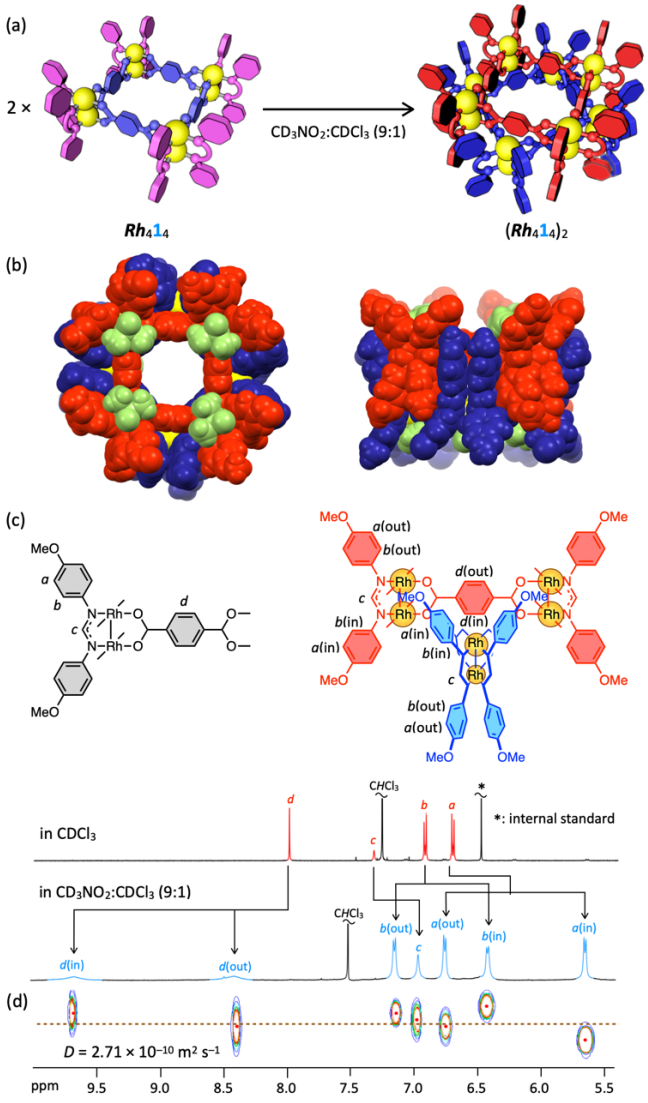

Figure 7. (a) Dimer formation of the $\boldsymbol{Rh}_4\mathbf{1}_4$ square by the solvophobic effect. (b) Crystal structure of $[\boldsymbol{Rh}_4\mathbf{1}_4(\text{dmso-}S)_4]_2$. Two $\boldsymbol{Rh}_4\mathbf{1}_4$ squares engaged each other are shown in red and blue. DMSO molecules axially coordinating to the Rh(II) centers are colored in green. (c) ^{1}H NMR spectra (500 MHz, 298 K, aromatic region) of $[\boldsymbol{Rh}_4\mathbf{1}_4]_2$ in $CD_3NO_2/CDCl_3$ (9:1 (v/v)) and $\boldsymbol{Rh}_4\mathbf{1}_4$ in $CDCl_3$. (d) ^{1}H DOSY spectrum of $[\boldsymbol{Rh}_4\mathbf{1}_4]_2$ in $CD_3NO_2/CDCl_3$ (9:1 (v/v)).

Conclusions

In conclusion, the self-assembly of the $\boldsymbol{Rh}_4L_4$ squares was controlled kinetically to produce the $\boldsymbol{Rh}_4L_4$ squares selectively assisted by monotopic carboxylate ligand (dcb^-), which prevents the cyclization of the $\boldsymbol{Rh}_3L_3(dcb)$ chain intermediate. This is the first example of selective formation of coordination squares under kinetic control in solution. The metastable yet kinetically highly stabilized $\boldsymbol{Rh}_3L_3$ triangles can be transformed into the $\boldsymbol{Rh}_4L_4$ squares with dcb^- under very mild condition. The kinetic control of the self-assembly was also affected by solvent. The conversion of the $\boldsymbol{Rh}_3L_3$ triangles assisted by dcb^- was blocked by DMSO. These results indicate that the energy landscape of the dinuclear Rh(II)-based coordination self-assembly can be tuned by the leaving ligand and the solvent. These basic knowledges would be applied to a wide range of Rh(II)-based metal-organic polyhedra (MOPs),[69–71] whose self-assembly is limited compared with MOPs composed of other transition metal ions owing to the relatively inert equatorial Rh(II)–carboxylate bonds. As Rh(II)-based MOPs possess high thermal and chemical stabilities and catalytic activity, they are expected as a platform of new materials, so exploring the novel structures of Rh(II)-based MOPs and their efficient self-assembly by modulation of the energy landscapes will make a great progress of this filed.

Author contributions

S.H. conceived the project. A.O. and N.S carried out the self-assembly of the $\boldsymbol{Rh}_4L_4$ squares and their characterizations by NMR measurements and QASAP. A.O. crystalized $[\boldsymbol{Rh}_4\mathbf{1}_4(\text{dmso-}S)_4]_2$ and its X-ray analysis. N.S. carried out solution study on dimerization of $\boldsymbol{Rh}_4\mathbf{1}_4$, the conversion of the $\boldsymbol{Rh}_3L_3$ triangles into the $\boldsymbol{Rh}_4L_4$ squares and model reactions of the ligand exchanges. S.H. prepared the manuscript and all authors discussed the results and commented on the manuscript.

Conflicts of interest

There are no conflicts to declare.

Acknowledgements

This work was supported by JSPS KAKENHI grant numbers 19H02731, 19K22196 and 21K18974 and the Asahi Glass Foundation.

References

1. F. Würthner, C.-C. You, C. R. Saha-Möller, Metallosupramolecular squares: from structure to function, *Chem. Soc. Rev.* **2004**, *33*, 133−146. DOI: 10.1039/B300512G
2. M. Fujita, J. Yazaki, K. Ogura, Preparation of a macrocyclic polynuclear complex, [(en)Pd(4,4'-bpy)]$_4$(NO$_3$)$_8$ (en = ethylenediamine, bpy = bipyridine), which recognizes an organic molecule in aqueous media. *J. Am. Chem. Soc.* **1990**, *112*, 5645−5647. DOI: 10.1021/ja00170a042
3. P. J. Stang, D. H. Cao, S. Saito, A. M. Arif, Self-Assembly of cationic, tetranuclear, Pt(II) and Pd(II) macrocyclic squares. X-ray crystal structure of [Pt^{2+}(dppp)(4,4'-bipyridyl)2$^-$OSO$_2$CF$_3$]$_4$. *J. Am. Chem. Soc.* **1995**, *117*, 6273−6283. DOI: 10.1021/ja00128a015
4. P. J. Stang, B. Olenyuk, J. Fan, A. M. Arif, Combining ferrocenes and molecular squares: Self-assembly of heterobimetallic macrocyclic squares incorporating mixed transition metal systems and a main group element. Single-crystal X-ray structure of [Pt(dppf)(H$_2$O)$_2$][OTf]$_2$. *Organometallics* **1996**, *15*, 904−908. DOI: 10.1021/om950781q
5. F. Würthner, A. Sautter, Highly fluorescent and electroactive molecular squares containing perylene bisimide ligands. *Chem. Commun.* **2000**, 445−446. DOI: 10.1039/A909892E
6. A. Sautter, B. K. Kaletaş, D. G. Schmid, R. Dobrawa, M. Zimine, G. Jung, I. H. M. van Stokkum, L. De Cola, R. M. Williams, F. Würthner, Ultrafast Energy-Electron Transfer Cascade in a Multichromophoric Light-Harvesting Molecular Square. *J. Am. Chem. Soc.* **2005**, *127*, 6719−6729. DOI: 10.1021/ja0448216
7. S.-S. Sun, A. J. Lees, Self-Assembly triangular and square Rhenium(I) tricarbonyl complexes: A comprehensive study of their preparation, electrochemistry, photophysics, photochemistry, and host−guest properties. *J. Am. Chem. Soc.* **2000**, *122*, 8956−8967. DOI: 10.1021/ja001677p
8. S. Kraft, E. Hanuschek, R. Beckhaus, D. Haase, W. Saak, Titanium-Based molecular squares and rectangles: Syntheses by self-assembly reactions of titanocene fragments and aromatic *N*-heterocycles. *Chem.–A Eur. J.* **2005**, *11*, 969−978. DOI: 10.1002/chem.200400880
9. F. A. Cotton, L. M. Daniels, C. Lin, C. A. Murillo, Square and triangular arrays based on Mo$_2^{4+}$ and Rh$_2^{4+}$ unit. *J. Am. Chem. Soc.* **1999**, *121*, 4538–4539. DOI: 10.1021/ja9901563
10. G.-H. Ning, L.-Y. Yao, L.-X. Liu, T.-Z. Xie, Y.-Z. Li, Y. Qin, Y.-J. Pan, S.-Y. Yu, Self-assembly and host−guest interaction of

metallomacrocycles using fluorescent dipyrazole linker with dimetallic clips. *Inorg. Chem.* **2010**, *49*, 7783−7792. DOI: 10.1021/ic100724r
11. R. V. Slone, D. I. Yoon, R. M. Calhoun, J. T. Hupp, Luminescent rhenium/palladium square complex exhibiting excited state intramolecular electron transfer reactivity and molecular anion sensing characteristics. *J. Am. Chem. Soc.* **1995**, *117*, 11813−11814. DOI: 10.1021/ja00152a027
12. S. M. Woessner, J. B. Helms, J. F. Houlis, B. Patrick Sullivan, Luminescent squares and rings based on metal-to-ligand charge transfer excited states. *Inorg. Chem.* **1999**, *38*, 4380−4381. DOI: 10.1021/ic9812813
13. S. Goeb, V. Prusakova, X. Wang, A. Vézinat, M. Sallé, F. N. Castellano, Phosphorescent self-assembled Pt^{II} tetranuclear metallocycles. *Chem. Commun.* **2011**, *47*, 4397−4399. DOI: 10.1039/C1CC10239G
14. D. E. Janzen, K. N. Patel, D. G. VanDerveer, G. J. Grant, Synthesis and structure of a platinum(II) molecular square incorporating four fluxional thiacrown ligands: The crystal structure of $[Pt_4([9]aneS_3)_4(4,4'\text{-bipy})_4](OTf)_8$. *Chem. Commun.* **2006**, 3540−3542. DOI: 10.1039/B606753K
15. X. Liu, C. L. Stern and C. A. Mirkin, Chemical origami: Formation of flexible 52-membered tetranuclear metallacycles via a molecular square formed from a hemilabile ligand. *Organometallics* **2002**, *21*, 1017−1019. DOI: 10.1021/om010964e
16. P. Teo, L. L. Koh, T. S. Andy Hor, Unusual coordination assemblies from platinum(II) thienyl and bithienyl complexes. *Inorg. Chem.* **2003**, *42*, 7290−7296. DOI: 10.1021/ic034690u
17. S. Karthikeyan, K. Velavan, R. Sathishkumar, B. Varghese, B. Manimaran, Self-assembly of manganese(I)-based molecular squares: Synthesis and spectroscopic and structural characterization. *Organometallics* **2012**, *31*, 1953−1957. DOI: 10.1021/om201244a
18. N. Sinha, F. Roelfes, A. Hepp, F. E. Hahn, Single-step synthesis of organometallic molecular squares from NR,NR′,NR″,NR‴-substituted benzobiscarbenes. *Chem. Eur. J.* **2017**, *23*, 5939−5942. DOI: 10.1002/chem.201604996
19. S. Pradhan, R. P. John, Self-assembled Pd_6L_4 cage and Pd_4L_4 square using hydrazide based ligands: Synthesis, characterization and catalytic activity in Suzuki–Miyaura coupling reactions. *RSC Adv.* **2016**, *6*, 12453−12460. DOI: 10.1039/C6RA00055J
20. J.-Y. Balandier, M. Chas, S. Goeb, P. I. Dron, D. Rondeau, A. Belyasmine, N. Gallego, M. Sallé, A self-assembled bis(pyrrolo)tetrathiafulvalene-based redox active square. *New J. Chem.* **2011**, *35*, 165−168. DOI: 10.1039/C0NJ00545B
21. P. Howlader, P. Bhandari, D. Chakraborty, J. K. Clegg, P. S. Mukherjee, Self-assembly of a Pd_8 macrocycle and Pd_{12} homochiral tetrahedral cages using poly(tetrazolate) Linkers. *Inorg. Chem.* **2020**, *59*, 15454−15459. DOI: 10.1021/acs.inorgchem.0c02452
22. M. Schweiger, S. R. Seidel, A. M. Arif, P. J. Stang, The self-assembly of an unexpected, unique supramolecular triangle composed of rigid subunits. *Angew. Chem. Int. Ed*. **2001**, *40*, 3467−3469. DOI: 10.1002/1521-3773(20010917)40:18<3467::AID-ANIE3467>3.0.CO;2-4
23. A. Sautter, D. G. Schmid, G. Jung, F. Würthner, A triangle−square equilibrium of metallosupramolecular assemblies based on Pd(II) and Pt(II) corners and diazadibenzoperylene bridging ligands. *J. Am. Chem. Soc.* **2001**, *123*, 5424−5430. DOI: 10.1021/ja004360y
24. M. Schweiger, S. R. Seidel, A. M. Arif, P. J. Stang, Solution and solid state studies of a triangle−square equilibrium: Anion-induced selective crystallization in supramolecular self-assembly. *Inorg. Chem.* **2002**, *41*, 2556−2559. DOI: 10.1021/ic0112692
25. M. Ferrer, M. Mounir, O. Rossell, E. Ruiz, M. A. Maestro, Equilibria between metallosupramolecular squares and triangles with the new rigid linker 1,4-bis(4-pyridyl)tetrafluorobenzene. Experimental and theoretical study of the structural dependence of NMR data. *Inorg. Chem.* **2003**, *42*, 5890−5899. DOI: 10.1021/ic034489j
26. S.-Y. Yu, H.-P. Huang, S.-H. Li, Q. Jiao, Y.-Z. Li, B. Wu, Y. Sei, K. Yamaguchi, Y.-J. Pan, H.-W. Ma, Solution self-assembly, spontaneous deprotonation, and crystal structures of bipyrazolate-bridged metallomacrocycles with dimetal centers. *Inorg. Chem.* **2005**, *44*, 9471−9488. DOI: 10.1021/ic0509332
27. L. A. Berben, M. C. Faia, N. R. M. Crawford, J. R. Long, Angle-dependent electronic effects in 4,4′-bipyridine-bridged Ru_3 triangle and Ru_4 square complexes. *Inorg. Chem.* **2006**, *45*, 6378−6386. DOI: 10.1021/ic060570l
28. F. A. Cotton, C. A. Murillo, R. Yu, Dynamic equilibrium between cyclic oligomers. Thermodynamic and structural characterization of a square and a triangle. *Dalton Trans.* **2006**, 3900−3905. DOI: 10.1039/B604928A
29. M. Ferrer, A. Gutiérrez, M. Mounir, O. Rossell, E. Ruiz, A. Rang, M. Engeser, Self-assembly reactions between the *cis*-protected metal corners $(N{-}N)M^{II}$ (N−N = ethylenediamine, 4,4′-substituted 2,2′-bipyridine; M = Pd, Pt) and the fluorinated edge 1,4-bis(4-pyridyl)tetrafluorobenzene. *Inorg. Chem.* **2007**, *46*, 3395−3406. DOI: 10.1021/ic062373s
30. Q.-F. Sun, K. M.-C. Wong, L.-X. Liu, H.-P. Huang, S.-Y. Yu, V. W.-W. Yam, Y.-Z. Li, Y.-J. Pan, K.-C. Yu, Self-assembly, structures, and photophysical properties of 4,4′-bipyrazolate-linked metallo-macrocycles with dimetal clips. *Inorg. Chem.* **2008**, *47*, 2142−2154. DOI: 10.1021/ic701344p
31. T. Weilandt, R. W. Troff, H. Saxell, K. Rissanen, C. A. Schalley, Metallo-supramolecular self-assembly: the case of triangle-square equilibria. *Inorg. Chem.* **2008**, *47*, 7588−7598. DOI: 10.1021/ic800334k
32. E. Holló-Sitkei, G. Tárkányi, L. Párkányi, T. Megyes, G. Besenyei, Steric effects in the self-assembly of palladium complexes with chelating diamine ligands. *Eur. J. Inorg. Chem.* **2008**, 2008, 1573−1583. DOI: 10.1002/ejic.200701189
33. S. Ghosh, P. S. Mukherjee, Self-assembled Pd(II) metallocycles using an ambidentate donor and the study of square−triangle equilibria. *Inorg. Chem.* **2009**, *48*, 2605−2613. DOI: 10.1021/ic802254f
34. M. Ferrer, A. Pedrosa, L. Rodríguez, O. Rossell, M. Vilaseca, New insights into the factors that govern the square/triangle equilibria of Pd(II) and Pt(II) supramolecules. Unexpected participation of a mononuclear species in the equilibrium. *Inorg. Chem.* **2010**, *49*, 9438−9449. DOI: 10.1021/ic101150p
35. M. H. Chisholm, N. J. Patmore, C. R. Reed, N. Singh, Oxalate bridged triangles Incorporating Mo_2^{4+} Units. Electronic structure and bonding. *Inorg. Chem.* **2010**, *49*, 7116−7122. DOI: 10.1021/ic1009237
36. J. Voignier, J. Frey, T. Kraus, M. Buděšínský, J. Cvačka, V. Heitz, J.-P. Sauvage, Transition-metal-complexed cyclic [3]- and [4]pseudorotaxanes containing rigid ring-and-filament conjugates: Synthesis and solution studies. *Chem. Eur. J.* **2011**, *17*, 5404–5414. DOI: 10.1002/chem.201003592
37. S. Goeb, S. Bivaud, P. I. Dron, J.-Y. Balandier, M. Chas, M. Sallé, A BPTTF-based self-assembled electron-donating triangle capable of C_{60} binding. *Chem. Commun.* **2012**, *48*, 3106−3108. DOI: 10.1039/C2CC00065B
38. R. Hashiguchi, K. Otsubo, H. Ohtsu, H. Kitagawa, A novel triangular macrocyclic compound, $[(tmeda)Pt(azpy)]_3(PF_6)_6{\cdot}13H_2O$ (tmeda: tetramethylethylenediamine, azpy: 4,4′-azopyridine). *Chem. Lett.* **2013**, *42*, 374−376. DOI: 10.1246/cl.121240
39. X.-F. Jiang, J.-H. Hu, J. Tong, S.-Y. Yu, Coexistence of molecular Pd_6 triangle and Pd_8 square self-assembled from naphthyl-dipyrazole with di-palladium motifs. *Inorg. Chem. Commun.* **2013**, *36*, 232−235. DOI: 10.1016/j.inoche.2013.09.012
40. G. Gupta, A. Das, K. C. Park, A. Tron, H. Kim, J. Mun, N. Mandal, K.-W. Chi, C. Y. Lee, Self-assembled novel BODIPY-based palladium supramolecules and their cellular localization. *Inorg. Chem.* **2017**, *56*, 4615−4621. DOI: 10.1021/acs.inorgchem.7b00260
41. B. Roy, R. Saha, A. K. Ghosh, Y. Patil , P. S. Mukherjee, Versatility of two diimidazole building blocks in coordination-driven self-assembly. *Inorg. Chem.* **2017**, *56*, 3579−3588. DOI: 10.1021/acs.inorgchem.7b00037
42. R. Saha, J. Sahoo, M. Venkateswarulu, M. De, P. S. Mukherjee, Shifting the triangle−square equilibrium of self-assembled metallocycles by guest binding with enhanced photosensitization. *Inorg. Chem.* **2022**, *61*, 17289−17298. DOI: 10.1021/acs.inorgchem.2c02920
43. D. A.Poole III, E. O. Bobylev, S. Mathew, J. N. H. Reek, Entropy directs the self-assembly of supramolecular palladium coordination macrocycles and cages. *Chem. Sci.* **2022**, *13*, 10141−10148. DOI: 10.1039/D2SC03154J
44. L. H. Foianesi-Takeshige, S. Takahashi, T. Tateishi, R. Sekine, A. Okazawa, W. Zhu, T. Kojima, K. Harano, E. Nakamura, H. Sato, S. Hiraoka, Bifurcation of self-assembly pathways to sheet or cage

controlled by kinetic template effect. *Commun. Chem.* **2019**, *2*, 128. DOI: 10.1038/s42004-019-0232-2
45. T. Tateishi, S. Takahashi, A. Okazawa, V. Martí-Centelles, J. Wang, T. Kojima, P. J. Lusby, H. Sato, S. Hiraoka, Navigated self-assembly of a Pd_2L_4 cage by modulation of an energy landscape under kinetic control. *J. Am. Chem. Soc.* **2019**, *141*, 19669−19676. DOI: 10.1021/jacs.9b07779
46. Y. Sakata, R. Yamamoto, D. Saito, Y. Tamura, K. Maruyama, T. Ogoshi, S. Akine, Metallonanobelt: A kinetically stable shape-persistent molecular belt prepared by reversible self-assembly processes. *Inorg. Chem.* **2018**, *57*, 15500−15506. DOI: 10.1021/acs.inorgchem.8b02804
47. M. J. Burke, G. S. Nichol, P. J. Lusby, Orthogonal selection and fixing of coordination self-assembly pathways for robust metallo-organic ensemble construction. *J. Am. Chem. Soc.* **2016**, *138*, 9308−9315. DOI: 10.1021/jacs.6b05364
48. S. Tashiro, M. Tominaga, T. Kusukawa, M. Kawano, S. Sakamoto, K. Yamaguchi, M. Fujita, Pd^{II}-directed dynamic assembly of a dodecapyridine ligand into end-capped and open tubes: The importance of kinetic control in self-assembly. *Angew. Chem., Int. Ed.* **2003**, *42*, 3267−3270. DOI: 10.1002/anie.200351397
49. L. Liu, G. Lyu, C. Liu, F. Jiang, D. Yuan, Q. Sun, K. Zhou, Q. Chen, M. Hong, Controllable reassembly of a dynamic metallocage: From thermodynamic control to kinetic control. *Chem. Eur. J.* **2017**, *23*, 456−461. DOI: 10.1002/chem.201604540
50. M. Yamanaka, Y. Yamada, Y. Sei, K. Yamaguchi, K. Kobayashi, Selective formation of a self-assembling homo or hetero cavitand cage via metal coordination based on thermodynamic or kinetic control. *J. Am. Chem. Soc.* **2006**, *128*, 1531−1539. DOI: 10.1021/ja0555365
51. A. Kumar, P. S. Mukherjee, Multicomponent self-assembly of Pd^{II}/Pt^{II} interlocked molecular cages: Cage-to-cage conversion and self-sorting in aqueous medium. *Chem. Eur. J.* **2020**, *26*, 4842−4849. DOI: 10.1002/chem.202000122
52. D. Preston, J. E. Barnsley, K. C. Gordon, J. D. Crowley, Controlled formation of heteroleptic $[Pd_2(L^a)_2(L^b)_2]^{4+}$ cages. *J. Am. Chem. Soc.* **2016**, *138*, 10578−10585. DOI: 10.1021/jacs.6b05629
53. F. A. Cotton, L. M. Daniels, C. Lin, C. A. Murillo, S.-Y. Yu, Supramolecular squares with Rh_2^{4+} corners. *J. Chem. Soc., Dalton Trans.* **2001**, 502−504. DOI: 10.1039/B009613J
54. R. P. Bonar-Law, T. D. McGrath, N. Singh, J. F. Bickley, A. Steiner, Dinuclear complexes as connectors for carboxylates. Self-assembly of a molecular box. *Chem. Commun.* **1999**, 2457−2458. DOI: 10.1039/A906415J
55. J. M. Casas, R. H. Cayton, M. H. Chisholm, Comments on the substitutional lability of the dimetal carboxylates of molybdenum and rhodium. Effects of M-M MO configuration. *Inorg. Chem.* **1991**, *30*, 358−360. DOI: 10.1021/ic00003a002
56. M. H. Chisholm, J. C. Huffman, S. S. Iyer, Some studies of the substitution chemistry of $[Rh_2(OAc)_2(CH_3CN)_4][BF_4]_2$ with monodentate and bidentate tertiary phosphines. *J. Chem. Soc., Dalton Trans.* **2000**, 1483−1489. DOI: 10.1039/B001444N
57. T. Yoshimura, K. Umakoshi, Y. Sasaki, Structural studies on the stepwise chelating processes of bidentate 2-(aminomethyl)pyridine and tridentate bis(2-pyridylmethyl)amine toward an acetate-bridged dirhodium(II) center. *Inorg. Chem.* **2003**, *42*, 7106−7115. DOI: 10.1021/ic030093w
58. S. Kai, Y. Sakuma, T. Mashiko, T. Kojima, M. Tachikawa, S. Hiraoka, The effect of solvent and coordination environment of metal source on the self-assembly pathway of a Pd(II)-mediated coordination capsule. *Inorg. Chem.* **2017**, *56*, 12652−12663. DOI: 10.1021/acs.inorgchem.7b02152
59. T. Abe, S. Horiuchi, S. Hiraoka, Kinetically controlled narcissistic self-sorting of Pd(ii)-linked self-assemblies from structurally similar tritopic ligands. *Chem. Commun.* **2022**, *58*, 10829−10832. DOI: 10.1039/D2CC04496J
60. M. M. Davis, H. B. Hetzer, Relative strengths of forty aromatic carboxylic acids in benzene at 25 °C. *J. Res. Natl. Bur. Stand.* **1958**, *60*, 569−592.
61. J. Jover, R. Bosque, J. Sales, QSPR prediction of pK_a for benzoic acids in different solvents. *QSAR Comb. Sci.* **2008**, *27*, 563−581.
62. Y. Tsujimoto, T. Kojima , S. Hiraoka, Rate-determining step in the self-assembly process of supramolecular coordination capsules. *Chem. Sci.* **2014**, *5*, 4167−4172. DOI: 10.1039/C4SC01652A
63. S. Hiraoka, Self-assembly processes of Pd(II)- and Pt(II)-linked discrete self-assemblies revealed by QASAP. *Isr. J. Chem.* **2019**, *59*, 151−165. DOI: 10.1002/ijch.201800073
64. S. Hiraoka, S. Takahashi and H. Sato, Coordination sf-assembly processes revealed by collaboration of experiment and theory: Toward kinetic control of molecular self-assembly. *Chem. Rec.* **2021**, *21*, 443−459. DOI: 10.1002/tcr.202000124
65. A. Baba, T. Kojima and S. Hiraoka, Self-assembly process of dodecanuclear Pt(II)-linked cyclic hexagon. *J. Am. Chem. Soc.* **2015**, *137*, 7664−7667. DOI: 10.1021/jacs.5b04852
66. A. Baba, T. Kojima, S. Hiraoka, Quantitative analysis of the self-assembly process of hexagonal Pt^{II} macrocyclic complexes: Effect of the solvent and the components. *Chem. Eur. J.* **2018**, *24*, 838−847. DOI: 10.1002/chem.201702955
67. P. Piraino, G. Bruno, G. Tresoldi, S. Lo Schiavo, P. Zanello, Chemical oxidation of binuclear rhodium(I) complexes with silver salts. Synthesis, x-ray crystal structure, and electrochemical properties of the rhodium $[Rh_2^{4+}]$ mixed-ligand complex $Rh_2(Form)_2(O_2CCF_3)_2(H_2O)_2.0.5C_6H_6$ (Form = *N,N'*-di-p-tolylformamidinate anion). *Inorg. Chem.* **1987**, *26*, 91−96. DOI: 10.1021/ic00248a019
68. S. Lo Schiavo, F. Nicolò, G. Tresoldi, P. Piraino, New dirhodium(II,II) species as building corner connectors for square molecular boxes. *Inorg. Chim. Acta* **2003**, *343*, 351−356. DOI: 10.1016/S0020-1693(02)01171-4
69. J. Zhao, X. Yan, Rh(II)-based metal–organic polyhedral. *Chem. Lett.* **2020**, *49*, 659–665. DOI: 10.1246/cl.200152
70. L. Chen, T. Yang, H. Cui, T. Cai, L. Zhang, C.-Y. Su, A porous metal–organic cage constructed from dirhodium paddle-wheels: synthesis, structure and catalysis. *J. Mater. Chem. A* **2015**, *3*, 20201–20209. DOI: 10.1039/C5TA05592J
71. S. Furukawa, N. Horike, M. Kondo, Y. Hijikata, A. Carné-Sánchez, P. Larpent, N. Louvain, S. Diring, H. Sato, R. Matsuda, R. Kawano, S. Kitagawa, Rhodium−organic cuboctahedra as porous solids with strong binding sites. *Inorg. Chem.* **2016**, *55*, 10843−10846. DOI: 10.1021/acs.inorgchem.6b02091